Olefinic vs Aromatic π−H Interaction: A Theoretical Investigation of the Nature of Interaction of First-row Hydrides with Ethene and Benzene

P. Tarakeshwar, Hyuk Soon Choi, and Kwang S. Kim*

Contribution from the National Creative Research Initiative Center for Superfunctional Materials, Department of Chemistry, Pohang University of Science and Technology, San 31, Hyojadong, Pohang 790-784, Korea

Received April 18, 2000. Revised Manuscript Received January 25, 2001

Abstract: The nature and origin of the π−H interaction in both the ethene (olefinic) and benzene (aromatic) complexes of the first-row hydrides (BH_3, CH_4, NH_3, H_2O, and HF) has been investigated by carrying out high level ab initio calculations. The results indicate that the strength of the π−H interaction is enhanced as one progresses from CH_4 to HF. Unlike conventional H-bonds, this enhancement cannot be simply explained by the increase in electrostatic interactions or the electronegativity of the atom bound to the π H-bonded proton. The contributions of each of the attractive (electrostatic, inductive, dispersive) and repulsive exchange components of the total binding energy are important. Thus, the inductive energy is highly correlated to the olefinic π−H interaction as we progress from CH_3 to HF. On the other hand, both electrostatic and inductive energies are important in the description of the aromatic π−H interaction. In either case, the contribution of dispersion energies is vital to obtain an accurate estimate of the binding energy. We also elaborate on the correlation of various interaction energy components with changes in geometries and vibrational frequencies. The red-shift of the ν_{Y-H} mode is highly correlated to the inductive interaction. The dramatic increase in the exchange repulsion energies of these π complexes as we progress from CH_4 to HF can be correlated to the blue-shift of the highly IR active out-of-plane bending mode of the π system.

1. Introduction

One of the major goals of chemistry in recent times has been the investigation and understanding of weak interactions,[1−5] because of their ubiquitous role in diverse fields ranging from biomolecular structure, molecular recognition, supramolecular chemistry, condensed matter, crystallography, reaction mechanisms, and so forth.[6−10] As a result, the conventional H-bond (**A**−**H**···**B**), wherein both the donor **A** and acceptor **B** are electronegative atoms, has been experimentally and theoretically characterized in fine detail.[11,12] These characterizations also include variants of the conventional H-bond like short strong H-bonds[10] and dihydrogen bonds. However, little is known about weak interactions involving π systems such as the $\pi-\pi$ and π−H interactions.[13,14]

π−H interactions involving π systems are interesting both from a practical and theoretical point of view.[13] This is because they can be used as model systems to examine the nature of hydrophobicity at the molecular level and help distinguish the limits of what should or should not be considered as "hydrogen bonds". Although a number of experimental studies of weak interactions involving π systems have invoked the π−H

* To whom correspondence should be addressed.

(1) *Molecular Interactions. From van der Waals to Strongly Bound Complexes*; Scheiner, S., Ed.; Wiley: Chichester, 1997; Hobza, P.; Zahradanik, R. *Intermolecular Complexes*; Academia: Prague, 1988.

(2) Stone, A. J. *The Theory of Intermolecular Forces*; Clarendon Press: Oxford, 1996.

(3) Desiraju, G. R.; Steiner, T. *Weak Hydrogen Bond*: *In Structural Chemistry and Biology*; Oxford: New York, 1999.

(4) Nishio, M.; Hirota, M.; Umezawa, Y. *The CH-π Interaction*; Wiley−VCH: New York, 1998.

(5) Müller-Dethlefs, K.; Hobza, P. *Chem. Rev.* **2000**, *100*, 143.

(6) Pratt, D. W. *Annu. Rev. Phys. Chem.* **1998**, *49*, 481.

(7) Koehl, P.; Levitt, M. *J. Mol. Biol.* **1999**, *293*, 1161; Sagui, C.; Darden, T. A. *Annu. Rev. Biophys. Biomol. Struct.* **1999**, *28*, 155; Bush, C. A.; Martin-Pastor, M.; Imberty, A. *Annu. Rev. Biophys. Biomol. Struct.* **1999**, *28*, 269.

(8) Gellman, S. H. *Chem. Rev.* **1997**, *97*, 1231; Mombaerts, P. *Science* **1999**, *286*, 707; Allewell, N. M.; Shi, D. H.; Morizono, H.; Tuchman, M. *Acc. Chem. Res.* **1999**, *32*, 885; Niemz, A.; Rotello, V. M. *Acc. Chem. Res.* **1999**, *32*, 44; Kaifer, A. E. *Acc. Chem. Res.* **1999**, *32*, 62; Kim, E.; Paliwal, S.; Wilcox, C. S. *J. Am. Chem. Soc.* **1998**, *120*, 11192; Cochran, J. E.; Parrot, T. J.; Whitlock, B. J.; Whitlock, H. W. *J. Am. Chem. Soc.* **1992**, *114*, 2269; Ren, T.; Jin, Y.; Kim, K. S.; Kim, D. H. *J. Biomol. Struct. Dyn.* **1997**, *15*, 401; Hong, B. H.; Lee, J. Y.; Cho, S. J.; Yun, S.; Kim, K. S. *J. Org. Chem.* **1999**, *64*, 5661.

(9) Braga, D.; Grepioni, F. *Coord. Chem. Rev.* **1999**, *183*, 19; Row, T. N. G. *Coord. Chem. Rev.* **1999**, *183*, 81; Allen, F. H.; Howard, J. A. K.; Hoy, V. J.; Desiraju, G. R.; Reddy, D. S.; Wilson, C. C. *J. Am. Chem. Soc.* **1996**, *118*, 4081.

(10) Cleland, W. W.; Kreevoy, M. M. *Science* **1994**, *264*, 1887; Cleland, W. W.; Frey, P. A.; Gerlt, J. A. *J. Biol. Chem.* **1998**, *273*, 25529; Warshel, A. *J. Biol. Chem.* **1998**, *273*, 27035; Kim, K. S.; Oh, K. S.; Lee, J. Y. *Proc. Natl. Acad. Sci. U.S.A.* **2000**, *97*, 6373; Oh, K. S.; Cha, S.-S.; Kim, D.-H.; Cho, H.-S.; Ha, N.-C.; Choi, G.; Lee, J. Y.; Tarakeshwar, P.; Son, H. S.; Choi, K. Y.; Oh, B.-H.; Kim, K. S. *Biochemistry* **2000**, *39*, 13891.

(11) Pimentel, G. C.; McClellan, A. C. In *The Hydrogen Bond*; Pauling, L., Ed.; Freeman: San Francicso, 1960; Jeffrey, J. A.; Saenger, W. *Hydrogen Bonding in Biological Structures*; Springer-Verlag, Berlin, 1991; Jeffrey, J. A. *Introduction to Hydrogen Bonding*; University Press: Oxford, 1997; Scheiner, S. *Hydrogen Bonding*: *A Theoretical Perspective*; University Press: Oxford, 1997.

(12) Del Bene, J. E. In *Encyclopedia of Computational Chemistry*; Schleyer, P. v. R., Ed.; John Wiley and Sons Inc.: New York, 1998; pp 1263−1271; Lii, J. H. In *Encyclopedia of Computational Chemistry*; Schleyer, P. v. R., Ed.; John Wiley and Sons Inc.: New York, 1998; pp 1271−1283; Stewart, J. J. P. In *Encyclopedia of Computational Chemistry*; Schleyer, P. v. R., Ed.; John Wiley and Sons Inc.: New York, 1998; pp 1283−1286.

(13) Kim, K. S.; Tarakeshwar, P.; Lee, J. Y. *Chem. Rev.* **2000**, *100*, 4145.

(14) Brutschy, B. *Chem. Rev.* **2000**, *100*, 3891.

10.1021/ja0013531 CCC: $20.00
Published on Web 03/20/2001

interactions to explain conformational preferences in organic and bio-molecules, crystal packing, host−guest complexation, it has been difficult to estimate their intrinsic stability in vivo.[15−19] Thus, theoretical calculations are the only recourse to obtain reliable estimates of their stability and understand their origin. However, the lack of detailed investigations of these interactions has given rise to different interpretations of the π H-bond with earlier studies attributing the formation of a π H-bond to be due to electrostatic interactions, with the π-cloud of the olefinic or aromatic system behaving as an electron donor or proton acceptor. As a result of this interpretation, the strength of the $\pi\cdots$HY interaction has been entirely correlated to the electronegativity of Y with the nature of the π system (olefinic or aromatic) having no role therein. Given the number of recent studies highlighting the importance of dispersive forces in governing the strength of interactions involving π systems, it becomes important to obtain a reliable estimate of the contributions of these individual interacting forces for π−H interactions of different π systems.[13] This detailed understanding of the physical origin of the π−H interaction, apart from resolving many of the misleading notions of the π−H interaction, would also aid the development of force-fields capable of accurately representing these interactions.

Most of the experimental studies of the π−H interaction are limited to the microwave and rotational investigations of the benzene complexes of NH_3, H_2O, and HF.[20−25] These investigations broadly indicate that as one progresses from $C_6H_6-NH_3$ to C_6H_6−HF there is a decrease in the intermolecular separation. Theoretical calculations of the binding energies of these benzene−HY complexes together with the observed decrease in the intermolecular separations seem to give an impression that the binding energies can be correlated to the electronegativity of the Y atom.[26,27] Although this is true to a limited extent, the high binding energies of the corresponding ethene complexes cannot be explained purely on the basis of the electronegativity of the Y atom. It becomes important to take into consideration the nature of the π system.

Most of the theoretical studies of π−H interactions carried out to date have only focused their attention on the evaluation of geometries and binding energies of these systems.[28−32] The few studies which have investigated the characteristics of both the olefinic and aromatic π−H interactions involve geometry optimizations at the Hartree−Fock level.[26,27] Since dispersive forces are important in the description of both the geometries and binding energies of these systems (as would be shown in subsequent sections), full geometry optimizations at the correlated levels are essential for the description of the π−H interactions.

In the course of our continuing interest in the properties of complexes containing π systems,[13] our objective in this theoretical study is to address some of the prevailing issues on the nature of the π−H interaction by evaluating the minimum energy geometries, binding energies, vibrational frequencies, charges, the complexes of the first-row hydrides (BH_3, CH_4, NH_3, H_2O, HF) with both the olefinic (ethene) and aromatic (benzene) π systems. These issues include (i) the strength of a π−H bond, (ii) the difference in the π−H interactions of olefinic and aromatic π systems, (iii) the modulation of the π−H interaction as a result of changes in the electronegativity of the atom attached to hydrogen, (iv) the changes in the individual energy components for different kinds of π−H interaction, (v) the correlation of either the binding energies or the individual energy components to the vibrational frequencies of these complexes, and (vi) a comparison of the π H-bond with the conventional hydrogen bond.

2. Methods

The interaction energy of van der Waals complexes has generally been calculated using two different approaches: the supermolecular method and computational methods based on the perturbative expansion of the energy in powers of the interaction operator.[33,34] Although the supermolecular method is conceptually simpler than perturbation theory, it does not provide any clear picture of the interaction. On the other hand, the interaction energy is directly calculated as a sum of perturbative corrections in the many-body implementation of the symmetry-adapted perturbation theory (SAPT).[34] A distinct advantage of SAPT over supermolecular calculations is that each correction term in the perturbation series can be physically interpreted.

Given the aims of the present study, we initially carried out conventional supermolecular (SM) calculations to evaluate the binding energies and vibrational frequencies of these complexes. Perturbational calculations using the SAPT program were then carried out to decompose the binding energy of these complexes into individual interaction energy components.[35] The details of the calculations are briefly elaborated to aid in the discussion of the results.

2.1. Supermolecular Calculations. A detailed conformational search was followed by a complete geometry optimization of all of these complexes at the second-order Møller−Plesset (MP2) level of theory using the 6-31+G* basis set.[29,36,37] After confirming that they were stable minima through evaluation of the vibrational frequencies at the MP2/6-31+G* level, the lowest-energy conformers obtained at the

(15) Ben-Naim, A. *Hydrophobic Interactions*; Plenum: New York, 1980; Tanford, C. *The Hydrophobic Effect: Formation of Micelles and Biological Membranes*; Wiley: New York, 1980.
(16) Muller, N. *Acc. Chem. Res*. **1990**, *23*, 23.
(17) Privalov, P.; Gill, S. J. *Adv. Protein Chem*. **1988**, *40*, 191; Burley, S. L.; Petsko, G. A. *Science* **1985**, *229*, 23.
(18) Kim, K. S.; Lee, J. Y.; Lee, S. J.; Ha, T.-K.; Kim, D. H. *J. Am. Chem. Soc*. **1994**, *116*, 7399; Lee, J. Y.; Lee, S. J.; Choi, H. S.; Cho, S. J.; Kim, K. S.; Ha, T.-K. *Chem. Phys. Lett*. **1995**, *232*, 67.
(19) Choi, H. S.; Suh, S. B.; Cho, S. J.; Kim, K. S. *Proc. Natl. Acad. Sci. U.S.A*. **1998**, *95*, 12094. Oh, K. S.; Lee, C.-W.; Choi, H. S.; Lee, S. J.; Kim, K. S. *Org. Lett*. **2000**, *2*, 2679.
(20) Baiocchi, F. A.; Williams, J. H.; Klemperer, W. *J. Phys. Chem*. **1983**, *87*, 2079.
(21) Suzuki, S.; Green, P. G.; Bumgarner, R. E.; Dasgupta, S.; Goddard, W. A.; Blake, G. A. *Science* **1992**, *257*, 942.
(22) Rodham, D. A.; Suzuki, S.; Suenram, R. D.; Lovas, F. J.; Dasgupta, S.; Goddard, W. A., III; Blake, G. A. *Nature* **1993**, *362*, 735.
(23) Gutowsky, H.; Emilson, T.; Arunan, E. *J. Chem. Phys*. **1993**, *99*, 4883.
(24) Peterson, K. I.; Klemperer, W. *J. Chem. Phys*. **1986**, *85*, 725.
(25) Andrews, A. M.; Kuczkowski, R. L. *J. Chem. Phys*. **1993**, *98*, 791.
(26) Cheney, B. V.; Schulz, M.; Cheney, J.; Richards, W. G. *J. Am. Chem. Soc*. **1988**, *110*, 4195; Cheney, B. V.; Schulz, M. *J. Phys. Chem*. **1990**, *94*, 6268.
(27) Brédas, J. L.; Street, G. B. *J. Chem. Phys*. **1989**, *90*, 7291.
(28) Kim, K. S.; Lee, J. Y.; Choi, H. S.; Kim, J.; Jang, J. H. *Chem. Phys. Lett*. **1997**, *265*, 497.
(29) Tarakeshwar, P.; Choi, H. S.; Lee, S. J.; Lee, J. Y.; Kim, K. S.; Ha, T.-K, Jang, J. H.; Lee, J. G.; Lee, H. *J. Chem. Phys*. **1999**, *111*, 5838.
(30) Feller, D. *J. Phys. Chem. A* **1999**, *103*, 7558.
(31) Tsuzuki, S.; Honda, K.; Uchimaru, T.; Mikami, M.; Tanabe, K. *J. Phys. Chem. A* **1999**, *103*, 8265.
(32) Tsuzuki, S.; Honda, K.; Uchimaru, T.; Mikami, M.; Tanabe, K. *J. Am. Chem. Soc*. **2000**, *122*, 3746.
(33) Chalasiński, G.; Szczęśniak, M. M. *Chem. Rev*. **1994**, *94*, 1723; Chalasiński, G.; Szczęśniak, M. M. *Chem. Rev*. **2000**, *100*, 4227.
(34) Jeziorski, B.; Moszynski, R.; Szalewicz, K. *Chem. Rev*. **1994**, *94*, 1887; Szalewicz, K.; Jeziorski, B. In *Molecular Interactions: From van der Waals to Strongly Bound Complexes*; Scheiner, S., Ed.; Wiley: New York, 1997; p 3.
(35) Jeziorski, B.; Moszyński, R.; Ratkiewicz, A.; Rybak, S.; Szalewicz, K.; Williams, H. L. In *Methods and Techniques in Computational Chemistry*: *METECC-94*; Clementi, E., Ed.; Vol. B, Medium Sized Systems; STEF: Cagliari, 1993; pp 79−129.
(36) Tarakeshwar, P.; Lee, S. J.; Lee, J. Y.; Kim, K. S. *J. Chem. Phys*. **1998**, *108*, 7217.
(37) Tarakeshwar, P.; Lee, S. J.; Lee, J. Y.; Kim, K. S. *J. Phys. Chem. B* **1999**, *103*, 184.

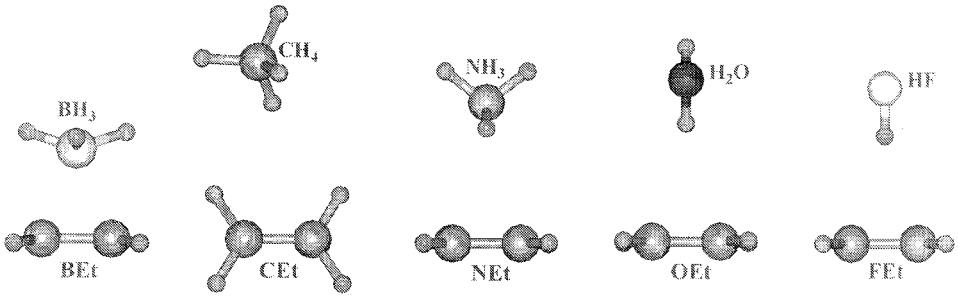

Figure 1. MP2/aug-cc-pVDZ optimized structures of all the ethene complexes.

MP2/6-31+G* level were subject to a full geometry optimization at the MP2/aug-cc-pVDZ level.[38] Vibrational frequencies were then evaluated on all the MP2/aug-cc-pVDZ optimized structures. Since the MP2/aug-cc-pVDZ method has been widely employed by us to investigate various intermolecular complexes, and seems to provide fairly accurate geometries and binding energies for a large number of complexes, this method has been employed in the present work.[13] In the case of the ethene complexes, single-point calculations at the coupled cluster singles doubles level of theory with noniterative inclusion of triples excitations {CCSD(T)}[39] were also carried out on the MP2/aug-cc-pVDZ optimized structures. All of the electrons were explicitly included in the correlation calculations.

The zero-point vibrational energy (ZPVE) corrections were computed from the frequencies evaluated at both the MP2/6-31+G* and MP2/aug-cc-pVDZ levels. The basis set superposition error (BSSE) corrections for the SM calculations were computed using the counterpoise method of Boys and Bernardi.[40] Our previous theoretical studies on benzene-containing complexes seem to suggest that a 100%-BSSE correction often underestimates the binding energies as compared to the experimentally determined energies, in particular for moderate-sized basis sets which are practical for the study of π-system-containing complexes. Hence we have often found it useful to employ a 50%-BSSE correction, the justification of which is given in a recent review.[13] All of the SM calculations reported in this study were carried out using the Gaussian suite of programs.[41]

The role of atomic charges in monitoring the changes in the electrostatic profiles of the individual monomers as a result of cluster-formation is well-known. In recent years, the natural bond orbital (NBO) analysis has been widely employed to evaluate the atomic charges,[42] because unlike most other charge-partitioning schemes, it is unaffected by the presence of diffuse functions in the basis set. The NBO charges reported in this study have been calculated using the densities obtained at the MP2 level.

2.2. SAPT Calculations. The Symmetry Adapted Perturbation Theory (SAPT) program[34,35] provides a rigorous quantitative quantum mechanical description of the intermolecular forces and also enables one to identify the physically meaningful terms originating from classical theories of intermolecular forces. Unlike most other decomposition procedures, SAPT allows for a natural description of the interaction energy in the form of a sum of *electrostatic*, *induction*, *dispersion*, and *exchange* interactions. One can also examine the changes obtained by step-by-step inclusion of electron correlation effects on these forces. In this study, the SAPT calculations were carried out using the geometry of the energy minimum (obtained from supermolecular calculations) of the complexes. The SAPT interaction energy accurate to third order, $E_{int}^{(SAPT)}$ is represented by $E_{int}^{(SAPT)} = E_{elst}^{(1)} + E_{exch}^{(1)} + E_{ind}^{(2)} + E_{exch-ind}^{(2)} + E_{disp}^{(2)} + E_{exch-disp}^{(2)} + \delta_{int}^{HF}$, where $E_{elst}^{(1)}$ is the electrostatic energy of the monomers with the unperturbed electron distribution, $E_{exch}^{(1)}$ is their first-order valence repulsion energy due to the Pauli exclusion principle, $E_{ind}^{(2)}$ stands for the second-order energy gain coming from the induction interaction, $E_{exch-ind}^{(2)}$ represents the repulsion change due to the electronic cloud deformation, $E_{disp}^{(2)}$ is the second-order dispersion energy, $E_{exch-disp}^{(2)}$ stands for the second-order correction for a coupling between the exchange repulsion and the dispersion interaction, and δ_{int}^{HF} includes the higher order induction and exchange corrections. The SAPT interaction energy can also be represented as the sum of $E_{int}^{(HF)}$ and $E_{int}^{(corr)}$, where $E_{int}^{(HF)}$ is the sum of all of the energy components evaluated at the Hartee−Fock level and $E_{int}^{(corr)}$ is the sum of all of the energy components evaluated at the correlated level. A detailed description of SAPT and some of its applications can be found in some recent references.[34,35,43−47]

3. Results and Discussion

To aid our discussion, we use the following notations: Et: C_2H_4, Bz: C_6H_6, B: BH_3, C: CH_4, N: NH_3, O: H_2O, F: HF. Thus for example, BEt denotes the complex $BH_3-C_2H_4$, and FBz denotes the complex $HF-C_6H_6$.

3.1. Geometries and Energetics. The geometries of all the π-complexes with the first-row hydrides shown in Figures 1 and 2 have been obtained after a detailed conformational search at the MP2/6-31+G* level.[29,36,37] The MP2/aug-cc-pVDZ binding energies and selected geometrical parameters of these structures are listed in Tables 1 and 2. It can be seen that both the **BEt** ($BH_3-C_2H_4$) and **BBz** ($BH_3-C_6H_6$) complexes do not allow a π−H interaction. The high binding energies observed therein emerge from the much stronger π-p_z interaction. The conformer of $BH_3-C_6H_6$ displaying a π−H interaction is nearly 3.3 kcal/mol higher in energy than the minimum energy conformer (**BBz**) at the MP2/6-31+G* level.[37] One of the major differences between the ethene and benzene π systems can be seen in their complexes with CH_4, with only conformer **CBz** ($CH_4-C_6H_6$) displaying the characteristics of a π−H interaction (hydrogen of CH_4 pointing toward the π-cloud of C_6H_6). The significant role of large basis sets in describing these complexes can be seen in the interactions of NH_3 with C_6H_6 (**NBz**).

(38) Dunning, T. H. *J. Chem. Phys.* **1989**, *90*, 1007.
(39) Crawford, T. D.; Schaefer, H. F., III. *Rev. Comput. Chem.* **2000**, *14*, 33.
(40) Boys, S. F.; Bernardi, F. *Mol. Phys.* **1970**, *19*, 553.
(41) Frisch, M. J.; Trucks, G. W.; Schlegel, H. B.; Gill, P. M. W.; Johnson, B. G.; Robb, M. A.; Cheeseman, J. R.; Keith, T. A.; Petersson, G. A.; Montgomery, J. A.; Raghavachari, K.; Al-Laham, M. A.; Zakrzewski, V. G.; Ortiz, J. V.; Foresman, J. B.; Cioslowski, J.; Stefanov, B. B.; Nanayakkara, A.; Chalcombe, M.; Peng, C. Y.; Ayala, P. Y.; Chen, W.; Wong, M. W.; Andres, J. L.; Replogle, E. S.; Gomperts, R.; Martin, R. L.; Fox, D. J.; Binkley, J. S.; Defrees, D. J.; Baker, J.; Stewart, J. P.; Head-Gordon, M.; Gonzalez, C.; Pople, J. A. *Gaussian 94*, revision A; Gaussian Inc.: Pittsburgh, PA, 1995.
(42) Reed, A. E.; Curtiss, L. A.; Weinhold, F. *Chem. Rev.* **1988**, *88*, 899.
(43) Moszyński, R.; Jeziorski, B.; Ratkiewicz, A.; Rybak, S. *J. Chem. Phys.* **1993**, *99*, 8856; Moszyński, R.; Jeziorski, B.; Rybak, S. *J. Chem. Phys.* **1994**, *100*, 1312. Moszyński, R.; Jeziorski, B.; Rybak, S.; Szalewicz, K.; Williams, H. L. *J. Chem. Phys.* **1994**, *100*, 5080. Rybak, S.; Jeziorski, B.; Szalewicz, K. *J. Chem. Phys.* **1995**, *95*, 6576. Moszyński, R.; Cybulski, S. M.; Chalasiński, G. *J. Chem. Phys.* **1994**, *100*, 4998. Chalasiński, G.; Jeziorski, B. *Theor. Chim. Acta* **1977**, *46*, 277. Moszyński, R.; Korona, T.; Wormer, P. E. S.; van der Avoird, A. *J. Phys. Chem. A* **1997**, *101*, 4690.
(44) Szalewicz, K.; Cole, S. J.; Kolos, W.; Bartlett, R. J. *J. Chem. Phys.* **1988**, *89*, 3662.
(45) Bukowski, R.; Szalewicz, K.; Chabalowski, C. *J. Phys. Chem. A* **1999**, *103*, 7322.
(46) Milet, A.; Moszynski, R.; Wormer, P. E. S.; van der Avoird, A. *J. Phys. Chem. A* **1999**, *103*, 6811.
(47) Wormer, P. E. S.; van der Avoird, A. *Chem. Rev.* **2000**, *100*, 4109.

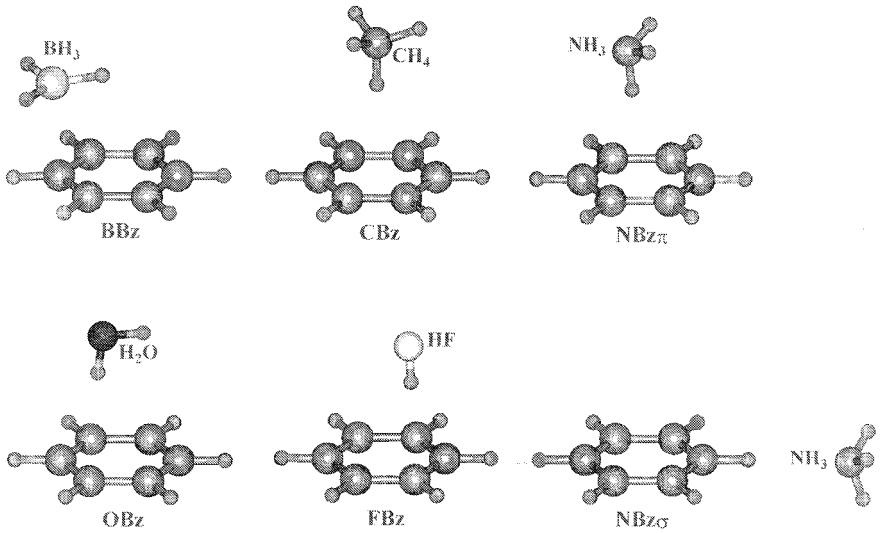

Figure 2. MP2/aug-cc-pVDZ optimized structures of all the benzene complexes.

Table 1: Binding Energies and Selected Distances of the Ethene Complexes[a]

	MP2/aug-cc-pVDZ[CCSD(T)/aug-cc-pVDZ][b]				
symmetry	**BEt** (C_s)	**CEt** (C_1)	**NEt** (C_1)	**OEt** (C_s)	**FEt** (C_s)
$-\Delta E_e^N$	14.45 [11.32]	1.45 [1.43]	2.22 [2.12]	3.43 [3.27]	5.47 [5.27]
$-\Delta E_e^B$	10.66 [7.54]	0.66 [0.65]	1.28 [1.15]	2.25 [2.02]	4.07 [3.74]
$-\Delta E_e$	12.56 [9.43]	1.06 [1.04]	1.75 [1.64]	2.84 [2.65]	4.77 [4.51]
$-\Delta E_o$	8.64 [5.51]	0.35 [0.34]	0.90 [0.78]	1.60 [1.42]	3.05 [2.79]
$-\Delta E_{cor}$	19.03 [15.90]	1.89 [1.87]	2.28 [2.18]	2.64 [2.49]	2.80 [2.60]
$-\Delta E_{es}$	0.58	0.19	1.46	3.11	5.76
$-\Delta H_{298}$	9.89	-0.17	0.47	1.47	3.55
$R_{H-\pi_{CM}}$	2.386	3.297	2.616	2.377	2.134
$R_{Y-\pi_{CM}}$	1.812	3.725	3.530	3.314	3.068
ΔR_{Y-H}	0.013	0.000	0.001	0.004	0.010
A	19941	24951	23909	23881	24416
B	13034	3406	3681	4085	4557
C	9574	3056	3301	3692	4057
μ	2.75	0.04	1.46	2.01	2.60

[a] Notations are as follows: **BEt** = ($BH_3-C_2H_4$), **CEt** = ($CH_4-C_2H_4$), **NEt** = ($NH_3-C_2H_4$), **OEt** = ($H_2O-C_2H_4$), **FEt** = ($HF-C_2H_4$). All energies are in kcal/mol; distances are in Å. "$-\Delta E_e^N$" and "$-\Delta E_e^B$" represent the binding energies without and with basis set superposition error (BSSE) correction, respectively. ΔE_e is chosen to represent the mid value of ΔE_e^N and ΔE_e^B as upper and lower bounds, respectively. ΔE_o is the ZPVE-corrected ΔE_e. In the case of CCSD(T), the ZPVE values evaluated at the MP2 level are used. ΔH_{298} is the enthalpy at 298.15 K and 1.0 atm. The frequencies for ZPE and thermal corrections were evaluated at the MP2/aug-cc-pVDZ level. The electron correlation energy ΔE_{cor} is the value of the E_e(MP2)/(CCSD(T)) subtracted by E_e(HF) at the MP2 optimized geometry. ΔE_{es} is the electrostatic (charge−charge) interaction energy evaluated using NBO charges. ΔH_{298} is the enthalpy at 298.15 K and 1.0 atm. $R_{H-\pi_{CM}}$ and $R_{Y-\pi_{CM}}$ are the distances from ethene center-of-plane to the H and Y (B, C, N, O, F) atoms, respectively. ΔR_{Y-H} is change observed in the Y−H bond distance upon complexation. A, B, C are the rotational constants in MHz respectively. μ is the dipole moment in Debye. [b] The CCSD(T)/aug-cc-pVDZ//MP2/aug-cc-pVDZ values are enclosed in square brackets.

Table 2: Binding Energies and Selected Distances of the Benzene Complexes at the MP2/aug-cc-pVDZ level[a]

	BBz	**CBz**	**NBZ$_\pi$**	**NBz$_\sigma$**	**OBz**	**FBz**
$-\Delta E_e^N$	7.92	3.71	4.45	2.65	5.09	6.11
$-\Delta E_e^B$	4.49	1.22	1.97	1.44	2.83	3.88
$-\Delta E_e$	6.20	2.46	3.21	2.04	3.96	4.99
$-\Delta E_o$	3.83	1.48	2.13	1.25[b]	2.87	3.78
$-\Delta E_{cor}$	11.75	5.25	5.05	1.89	4.39	3.85
$-\Delta E_{es}$	0.36	0.57	3.18	2.51	6.90	9.67
$-\Delta H_{298}$	4.25	0.95	1.67	1.21	2.47	3.83
$R_{H-\pi_{CM}}$	2.656	2.429	2.362	5.494/5.395[c]	2.353	2.284
$R_{Y-\pi_{CM}}$	2.878	3.525	3.383	4.988	3.281	3.167
$\Delta R_{N-\pi_H}$	-	-	-	2.482	-	-
ΔR_{Y-H}	0.002	−0.001	0.001	0.001	0.003	0.007
A	3676	2754	2787	5457	2817	2937
B	2633	1954	2026	1124	2068	2052
C	2109	1953	2012	937	2059	1984
μ	1.55	0.20	1.57	2.23	2.24	2.45

[a] All energies are in kcal/mol; distances are in Å. All the complexes possess C_s point group symmetry. $R_{H-\pi_{CM}}$ and $R_{Y-\pi_{CM}}$ are the distances from benzene center-of-plane to the H and Y (B, C, N, O, F) atoms, respectively. $R_{N-\pi_H}$ is the distance from the hydrogen-bonded benzene hydrogen to the nitrogen of ammonia. See footnotes of Table 1 for other definitions. [b] Single imaginary frequency neglected in the evaluation of ZPVE. [c] First distance occurs twice, second occurs once.

Calculations using small basis sets (6-31+G*) lead to the sigma conformer (**NBz**$_\sigma$) being energetically more favored than the corresponding π (**NBz**$_\pi$) conformer. However at the MP2/aug-cc-pVDZ level, conformer **NBz**$_\pi$ is energetically more favored, which is in line with the experimental observations.[22]

In recent theoretical studies we had described the efficacy of the MP2/aug-cc-pVDZ method in describing the geometries and energetics of intermolecular complexes exhibiting the $\pi-$H interaction.[29,48] The MP2/aug-cc-pVDZ geometries of these complexes indicate that there is a gradual elongaton of the R_{Y-H} (Y= C, N, O, F) distance as one progresses from CH_4 to HF, with the effect being more pronounced in the complexes formed with HF. The $R_{H-\pi_{CM}}$ distances (π_{CM} denotes center-of-mass of the π system), on the other hand, indicate that the intermolecular separation of the hydride and the π system decreases on moving from CH_4 to HF, with the decrease being more pronounced in the ethene than in the benzene complexes. Upon complexation little changes (with the exception of the complexes of BH_3) are observed in the geometries of the π system and the hydride.

The binding energies of these $\pi-$H complexes evaluated at the MP2/aug-cc-pVDZ are in general in good agreement with the experimental binding energies.[28,29] However, it should be noted that wide-ranging zero vibrational effects have to be taken into account to obtain very accurate estimates of the binding energies of these complexes.[28] A plot of the ZPVE corrected binding energies of these complexes (Figure 3) evaluated at the MP2/aug-cc-pVDZ level reveals that the ethene complexes have lower binding energies when compared to those of the corre-

(48) Tarakeshwar, P.; Kim, K. S.; Brutschy, B. *J. Chem. Phys.* **2000**, *112*, 1769; Tarakeshwar, P.; Kim, K. S.; Brutschy, B. *J. Chem. Phys.* **2001**, *114*, 1295; Tarakeshwar, P.; Kim, K. S.; Djafari, S.; Buchhold, K.; Reimann, B.; Barth, H.-D.; Brutschy, B. *J. Chem. Phys.* **2001**, *114*, 4016.

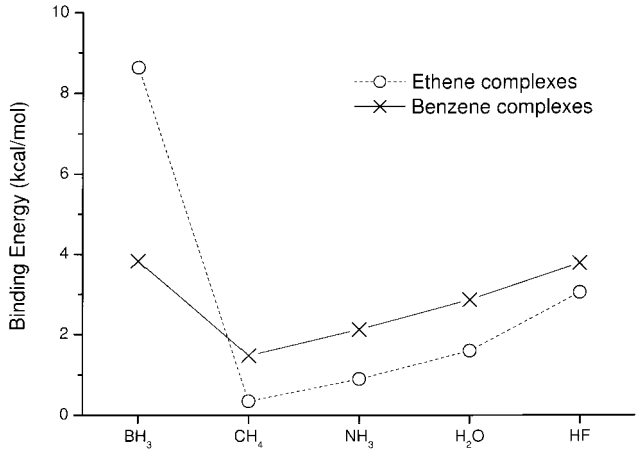

Figure 3. Comparison of the BSSE and ZPVE corrected binding energies (MP2/aug-cc-pVDZ) of all the ethene and benzene complexes.

sponding benzene complexes. The rough estimates of the correlation (ΔE_{cor}) and electrostatic (ΔE_{es})[49] energies reveal that in case of the ethene complexes, there is a gradual increase in both the correlation and electrostatic energies as one progresses from CH_4 to HF. On the other hand, in the benzene complexes, the dramatic increase in the electrostatic contribution is accompanied by a slight decrease in the correlation contribution.

Given the importance of correlation energies in the description of these complexes, it is useful to examine the consequences of employing higher levels of correlation in evaluating the binding energies. The CCSD(T) binding energies of the ethene complexes are similar to the corresponding MP2 binding energies, with the exception of the $C_2H_4-BH_3$ complex. This finding reinforces our earlier observations that the MP2/aug-cc-pVDZ method is adequate in the description of the $\pi-H$ interaction exhibited by these complexes. A similar observation was made in a very recent paper by Tsuzuki et al. on the interaction of methane with benzene.[32]

One of the popular methods of the decomposition of the binding energy of an intermolecular complex has been the Morokuma partitioning scheme.[50] One of the drawbacks of this scheme is that it is defined within the Hartree−Fock framework. Hence, this scheme cannot be employed for these π system-containing complexes, wherein electron correlation is important. In a recent paper, Tsuzuki et al. have tried to estimate some of the components, not available within the Morokuma partitioning scheme, using empirical models.[32] However, given the complex nature of these interactions, a partitioning scheme which explicitly takes into account electron correlation should be employed to obtain the individual energy components. Recently, we have shown that the decomposition of binding energies of weak van der Waals complexes containing π systems using SAPT provides a physical insight of the nature of interactions.[29,48]

The results of SAPT calculations carried out on all of the ethene-containing complexes using large basis sets and high levels of correlation are listed in Table 3. This table shows that the use of large basis sets and high levels of correlation only leads to an increase in the dispersion energies ($E_{disp}^{(2)}$). The extremely large size of the benzene complexes precludes the use of large basis sets and high levels of correlation in SAPT calculations. Hence, the interaction energy components of the benzene complexes obtained using the 6-31+G* basis set are listed in Table 4. The importance of the inclusion of electron correlation in the description of these complexes can be seen in the values of $E_{int}^{(corr)}$. Thus, the exclusion of $E_{int}^{(corr)}$ from the total interaction energy ($E_{int}^{(SAPT)}$) of these π complexes leads to either repulsive (complexes of CH_4 and NH_3) or diminished (complexes of H_2O and HF) interactions at the Hartee−Fock level. One can also note the significant difference between these complexes and that of the water dimer (an example of a conventional H-bond) from the values of $E_{int}^{(corr)}$.

An analysis of the origin of the $\pi-H$ interaction of the ethene complexes in terms of the contributions of the attractive energy components to the total attractive energy reveals that electrostatic energies ($E_{elst}^{(1)}$) contribute to less than 50% (~40% when one employs the aug-cc-pVDZ basis set) of the total *attractive* interaction in all these complexes. Additionally the percentage of the electrostatic contribution is nearly invariant as one progresses from NH_3 to HF. Furthermore, one also notes that the contribution of the higher-order exchange and induction corrections (δ_{int}^{HF}) is nearly uniform in all of the complexes. The contribution of the induction energy ($E_{ind}^{(2)}$) to the total attractive interaction, which is independent of the size of the basis-set, dramatically increases from about 20% in the **NEt** ($NH_3-C_2H_4$) complex to nearly 40% in the **FEt** ($HF-C_2H_4$) complex. This increase in the contribution of the induction energy can be attributed to the increased distortion of the electron cloud of the π system by the electric field of the hydride as we progress from NH_3 to HF. Although the magnitude of the dispersion energies is slightly higher in **FEt** than in **NEt**, the percentage of its contribution to the total attractive interaction is markedly lower. Thus, the contribution of inductive energies ($E_{ind}^{(2)}$) becomes more significant in going from CH_4 to HF.

A similar analysis of the contributions of the attractive energy components of the benzene complexes reveals an increase in both the contributions of the electrostatic and inductive energies as one progresses from CH_4 to HF. Nevertheless, we find a clear distinction between olefinic and aromatic $\pi-H$ interactions as shown in the following discussion.

The trends of various energy components, their sums, spectral shifts, and selected geometrical parameters of both the ethene and benzene complexes are shown in Figure 4. Figure 4a depicts the exchange energies [evaluated as the sum of the exchange ($E_{exch}^{(2)}$), exchange-induction ($E_{exch-ind}^{(2)}$), exchange-dispersion ($E_{exch-disp}^{(2)}$), and δ_{int}^{HF}]. The increase in the repulsive exchange energies is more pronounced in the ethene complexes than in the benzene complexes. The reason for the anomalous behavior of the exchange energies in case of the ethene and benzene complexes lies in both the size of the donor (hydride) and the way it approaches the π system. As we progress from CH_4 to HF, the decrease in the electron density of the H-atoms involved in the $\pi-H$ interaction leads to a closer approach to the π system because of a decrease of exchange repulsion at a given separation. Furthermore, the widely differing electron density profiles of the π cloud of benzene and ethene governs the approach of the hydride. The complexes with benzene are very different from those with ethene because the hydride aims at the midpoint of the ring (where there are no nuclei or bonds). Consequently, the decrease of the intermolecular $R_{Y-\pi_{CM}}$ distance with the decrease of the donor size would be smaller for the benzene than for the ethene complexes (Figure 4j). The

(49) The rough estimate of the electrostatic energy (ΔE_{es}), which is obtained using Coulomb's law and the NBO charges, should not be confused with the electrostatic energy ($E_{elst}^{(1)}$) obtained using SAPT.

(50) Morokuma, K. *J. Chem. Phys.* **1971**, *55*, 1236; Morokuma, K.; Kitaura, K. *Int. J. Quantum. Chem.* **1976**, *10*, 325; Morokuma, K.; Kitaura, K. In *Chemical Applications of Electrostatic Potentials*; Politzer, P., Truhlar, D. G., Eds.; Plenum: New York, 1981; pp 215−242.

Table 3: SAPT Interaction Energy Components of All the Ethene Complexes Obtained at the MP2 Level using both the 6-31+G* and aug-cc-pVDZ Basis Sets[a]

	6-31+G*					aug-cc-pVDZ				
	CEt	NEt	OEt	FEt	$(H_2O)_2$	CEt	NEt	OEt	FEt	$(H_2O)_2$
$E_{int}^{(SAPT)\,b}$	−0.13(−0.16)	−0.86(−0.92)	−1.70(−1.84)	−3.61(−3.88)	−4.61(−4.56)	−0.70(−0.73)	−1.20(−1.34)	−2.01(−2.31)	−3.84(−4.31)	−4.06(−4.38)
$E_{int}^{(corr)\,c}$	−0.48(−0.51)	−0.75(−0.81)	−0.74(−0.89)	−0.48(−0.75)	−0.16(−0.11)	−1.40(−1.42)	−1.42(−1.60)	−1.30(−1.56)	−0.92(−1.39)	−0.41(−0.73)
$E_{elst}^{(1)}$	−0.42(−0.40)	−2.14(−2.07)	−4.03(−3.90)	−6.77(−6.62)	−10.10(−9.82)	−0.62(−0.59)	−2.20(−2.12)	−3.91(−3.78)	−6.54(−6.41)	−8.41(−8.25)
$E_{exch}^{(1)}$	0.85(0.82)	2.58(2.48)	4.74(4.50)	8.03(7.62)	8.99(9.23)	1.54(1.57)	3.33(3.15)	5.45(5.12)	8.92(8.42)	8.47(8.60)
$E_{ind}^{(2)}$	−0.14(−0.14)	−0.79(−0.80)	−2.26(−2.25)	−5.57(−5.41)	−3.03(−3.62)	−0.18(−0.21)	−1.04(−1.04)	−2.66(−2.62)	−6.33(−6.09)	−2.90(−3.43)
$E_{disp}^{(2)}$	−0.53(−0.55)	−1.02(−1.05)	−1.37(−1.41)	−1.69(−1.76)	−1.47(−1.67)	−1.63(−1.72)	−2.03(−2.07)	−2.43(−2.54)	−2.85(−3.05)	−2.25(−2.63)
$E_{exch-ind}^{(2)}$	0.12(0.12)	0.58(0.58)	1.54(1.53)	3.43(3.33)	1.68(2.00)	0.15(0.17)	0.76(0.76)	1.80(1.77)	3.91(3.76)	1.55(1.82)
$E_{exch-disp}^{(2)}$	0.06	0.15	0.24	0.32	0.31	0.13	0.28	0.41	0.53	0.41
δ_{int}^{HF}	−0.06	−0.22	−0.55	−1.36	−0.98	−0.09	−0.3	−0.66	−1.48	−0.93

[a] All energies are in kcal/mol. [b] $E_{int}^{(SAPT)} = E_{elst}^{(1)} + E_{exch}^{(1)} + E_{ind}^{(2)} + E_{disp}^{(2)} + E_{exch-ind}^{(2)} + E_{exch-disp}^{(2)} + \delta_{int}^{HF}$. The energy components inside the parentheses have been evaluated at the CCSD level (for the exchange energies) and at the MP4 level (electrostatic and dispersion energies). [c] $E_{int}^{(corr)}$ is the sum of all the energy components evaluated at the correlated level.

Table 4: MP2 Equivalent SAPT Interaction Energy Components of All the Benzene Complexes Obtained using the 6-31+G* Basis Set[a]

	CBz	**NBZ$_\pi$**	**NBz$_\sigma$**	**OBz**	**FBz**
$E_{int}^{(SAPT)}$	−0.56	−1.27	−1.29	−2.23	−3.35
$E_{int}^{(corr)}$	−1.67	−1.67	−0.84	−1.33	−0.98
$E_{elst}^{(1)}$	−1.01	−2.22	−3.61	−3.51	−4.48
$E_{exch}^{(1)}$	2.41	3.30	4.54	4.09	5.40
$E_{ind}^{(2)}$	−0.49	−0.85	−1.31	−1.43	−3.43
$E_{disp}^{(2)}$	−1.96	−2.14	−1.34	−2.1	−2.00
$E_{exch-ind}^{(2)}$	0.39	0.59	0.64	0.8	1.69
$E_{exch-disp}^{(2)}$	0.24	0.27	0.24	0.26	0.25
δ_{int}^{HF}	−0.14	−0.23	−0.45	−0.34	−0.78

[a] All energies are in kcal/mol. See the footnotes of Table 3 for other notations.

smaller variation of $R_{Y-\pi_{CM}}$ in the benzene complexes also explains the near constancy of the dispersion energies ($E_{disp}^{(2)}$) (Figure 4b). On the other hand, the somewhat smaller decrease of $R_{Y-\pi_{CM}}$ in the ethene complexes, as we progress from CH_4 to HF, explains the slight increase in the dispersion energies (Figure 4b). It should be noted that the change in dispersion energy is governed by two factors: intermolecular separation and the electron population involved in the $\pi-H$ interaction (i.e., electron density around the π-bonded H atom). Given the larger electronegativity of F over that of C, the electron density around the hydrogen in CH_4 would be slightly higher than in HF. This can be partially evidenced from the charges of the hydrogen atoms shown in Table 5. Hence for a given intermolecular distance, the dispersion energy would be slightly higher for complexes involving CH_4 than HF.

A comparison of the electrostatic ($E_{elst}^{(1)}$) and inductive ($E_{ind}^{(2)}$) components of the ethene and benzene complexes plotted in Figure 4 f and g reveals that, in the case of complexes involving CH_4 and NH_3, their magnitudes are comparatively smaller for the ethene complexes. However, with the progressive decrease in the hydride size, the magnitude of these components in the ethene complexes is larger than the magnitudes observed in the corresponding benzene complexes. This behavior of the attractive inductive energies ($E_{ind}^{(2)}$) can be explained using an analogy of the cation-π interactions. In the case of the interactions of these π systems with organic cations such as tetramethylammonium (NMe_4^+), we had shown that a significant part of the binding energy emerges from the $\pi-\sigma^*$ interaction, which is of the inductive type.[18] What is however more important is that this inductive $\pi-\sigma^*$ interaction gets magnified at the MP2 level.[18,51] Thus, the inclusion of electron correlation is an important prerequisite for the magnification of these inductive interactions.

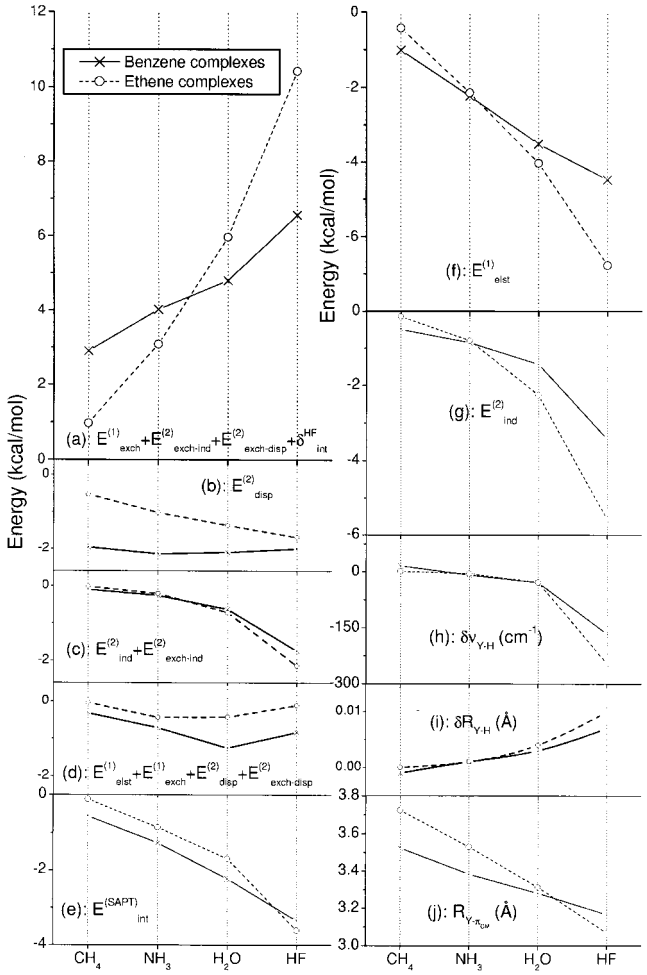

Figure 4. Comparison of the trends of the various interaction energy components and their sums (a−g), selected vibrational frequency shifts ($\delta\nu_{Y-H}$) (h), and geometrical parameters (δR_{Y-H}, $\delta R_{Y-\pi_{CM}}$) (i, j) of all the ethene and benzene complexes. The interaction energy components were obtained at a level equivalent to the supermolecular MP2/6-31+G*. See Table 3 for description of the notations. The geometrical parameters and frequency shifts were obtained at the MP2/aug-cc-pVDZ level.

To reinforce the arguments put forward in our analysis of the attractive energy components of these complexes, we have

(51) Minoux, H.; Chipot, C. *J. Am. Chem. Soc.* **1999**, *121*, 10366.

Table 5: MP2/aug-cc-pVDZ NBO Charge Shifts (au) of the Y (B, C, N, O, F) and H Atoms Interacting with the π System in All the Complexes[a]

atom	BH_3	CH_4	NH_3	H_2O	HF
		Ethene Complexes			
Y	−0.576	−0.004	−0.006	−0.010	−0.021
H	0.084/0.141[b]	0.000	0.003	0.004	0.001
		Benzene Complexes			
Y	−0.188	0.007	0.005	0.000	−0.009
H	0.034/0.029[b]	−0.007	−0.006	−0.003	0.001

[a] All shifts evaluated with respect to the charges observed in the corresponding monomers. [b] Since BH_3 does not form a π-H bond with either Et or Bz, the charge shifts of all its hydrogens are listed in case of the BH_3 complexes. First charge occurs once, second occurs twice.

plotted the sums of some of the energy components of both the ethene and benzene complexes in Figure 4 c and d. In the case of the ethene complexes, the sum of the electrostatic ($E^{(1)}_{elst}$), exchange ($E^{(2)}_{exch}$), dispersion ($E^{(2)}_{disp}$), and exchange-dispersion ($E^{(2)}_{exch-disp}$) energies is almost zero. Hence the trend of the total SAPT interaction energy ($E^{(SAPT)}_{int}$) of the ethene complexes shown in Figure 4e is similar to the trends exhibited by both the inductive ($E^{(2)}_{ind}$) (Figure 4g) and the sum of the inductive and exchange-induction ($E^{(2)}_{exch-ind}$) energies (Figure 4c). On the other hand, the total SAPT interaction energy of the benzene complexes (Figure 4e) can be correlated to the electrostatic ($E^{(1)}_{elst}$) (Figure 4f) and partially to inductive energies ($E^{(2)}_{ind}$) or the sum of ($E^{(2)}_{ind}$) and ($E^{(2)}_{exch-ind}$) (Figure 4 c, g).

To compare these results with those obtained for the water dimer (a representative of conventional H-bonding), we have listed the values obtained with the aug-cc-pVDZ basis set in Table 3. It can readily be seen that the binding energy of **OEt** ($H_2O-C_2H_4$) (wherein one of the water molecules is substituted with an ethene) is nearly half of that of the water dimer. The analysis of the attractive components of the interaction energy of the water dimer in Table 3 reveals that contribution of electrostatic energy to the total attractive interaction is much higher than in **OET** (∼60 vs ∼40%). Consequently the contributions of induction and dispersion energies to the total attractive interaction of the water dimer are much lower than in **OEt**. In case of **FEt** (C_2H_4-HF), whose binding energy is similar to that of the water dimer, the contribution of the dispersion energies to the total attractive interaction is similar. However, the decreased electrostatic contribution in **FEt** (∼1.8 kcal/mol) is compensated by a concurrent increase in the contribution of the induction energy (∼2.7 kcal/mol) and the dispersion energy (∼0.4 kcal/mol). It should be noted that the exchange energies (∼1.3 kcal/mol) are lower in the water dimer. The relatively smaller magnitude of the inductive energies as compared to the electrostatic energies is in agreement with the arguments put forward by Davidson and co-workers in their investigation of the water dimer.[52]

To further distinguish the conventional H-bond and the π H-bond, we have investigated the changes in the magnitude of the energy components as the intermolecular separation is slowly decreased from very larger separations.[53] In Figure 5, we have plotted the components for various intermolecular separations of the **OEt** ($H_2O-C_2H_4$) and **FEt** ($HF-C_2H_4$)

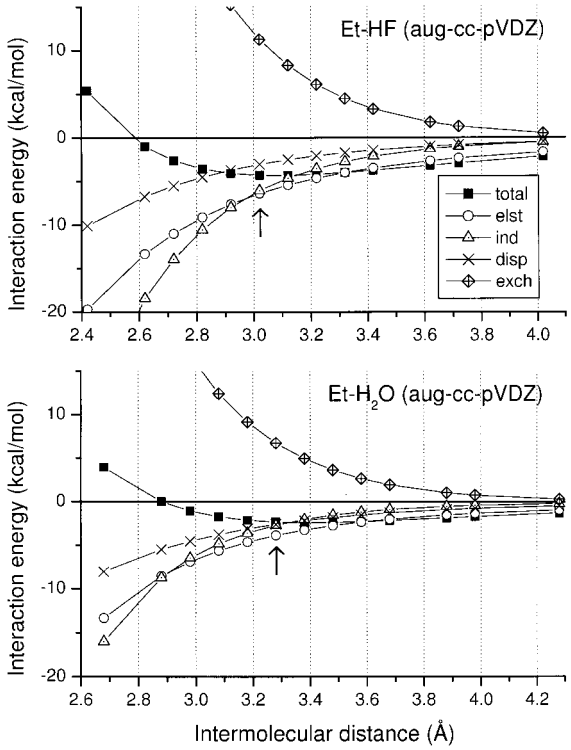

Figure 5. Comparison of the calculated SAPT interaction energy components of complex **OEt** and **FEt** at the aug-cc-pVDZ level. The exchange energies (exch) are the sum of all the exchange components ($E^{(2)}_{exch}$, $E^{(2)}_{exch-ind}$, δ^{HF}_{int}). The total energy is the sum of the electrostatic (elst:$E^{(1)}_{elst}$), inductive (ind:$E^{(2)}_{ind}$), dispersive (disp:$E^{(2)}_{disp}$), and exchange energies. The arrows indicate the equilibrium geometry.

complexes. The magnitude of the repulsive exchange energies has a far more important role in the characterization of the equilibrium geometry than the magnitude of the attractive energies such as electrostatic, inductive, and dispersive energies. In the case of complex **FEt**, the magnitude of inductive energy sharply increases and is larger than the dispersion energy even before the onset of the equilibrium geometry. Furthermore, at intermolecular separations smaller than those observed in the equilibrium geometry, their magnitude is higher than that of the electrostatic energy. On the other hand, in complex **OEt**, the magnitude of inductive energy becomes larger than the dispersion energy only at intermolecular separations smaller than those observed in the equilibrium geometry. In both **OEt** and **FEt** complexes, the difference in the magnitude of the electrostatic and the other attractive energies such as dispersion and inductive energies at various intermolecular separations is much smaller than that observed in case of the water dimer.[44]

3.2. Charges and Electron Density Shifts. The formation of a conventional H-bond normally results in subtle shifts of the electron density.[11] Even though these shifts are relatively small in magnitude, they have been found to be useful in the identification of such bonds. This electron density is drawn not only from the lone pair of the acceptor molecule participating in the H-bond but from the entire molecule. Consequently, the density rather than being localized over a particular region delocalizes throughout the donor molecule. Table 5, which lists the NBO charges of the hydrogen and the "Y" (Y = B, C, O, N, F) atom evaluated at the MP2/aug-cc-pVDZ level indicates that only the complexes of HF exhibit significant charge transfer, with the fluorine atom becoming more negative. This facet is also evident from the high electrostatic ($E^{(1)}_{elst}$) energies exhib-

(52) Ghanty, T. K.; Staroverov, V. N.; Koren, P. R.; Davidson, E. R. *J. Am. Chem. Soc*. **2000**, *122*, 1210.

(53) It is important to point out that in the evaluation of these energy components, the monomer geometries in the equilibrium geometry of the complex were employed. We have observed that this approximation has very little effect on the evaluated interaction energy components.

Table 6: Calculated Frequency Shifts of the Y−H Stretching Modes in All the Complexes at the MP2/aug-cc-pVDZ Level[a]

8.0qBEt	CEt	NEt	OEt	FEt
−79.0(142)	1.3(24)	−4.5(5)	−28.3(150)	−245.3(709)
−150.3(53)	−2.0(15)	−8.4(32)	−45.6(122)	
−72.4(23)	−3.9(17)	−7.2(14)		
	−2.0(0)			

BBz	CBz	NBz_π	NBz_σ	OBz	FBz
−30.4(100)	16.0(3)	−8.4(4)	−6.1(7)	−29.1(101)	−166.0(465)
−46.4(108)	−9.0(16)	−10.8(37)	−6.3(7)	−30.6(74)	
−29.6(21)	−9.0(16)	−7.5(8)	−5.0(3)		
	−2.8(7)				

[a] All frequencies are in cm^{-1}, and the IR intensities (km/mol) are enclosed in parantheses beside them.

ited by these complexes. Expectedly, the amount of charge gained by the "Y" atom can be correlated to its electronegativity. In the ethene complexes, the "Y" atom gains more negative charge than in the corresponding benzene complexes. This is, however, in contrast to the charges exhibited by the hydrogen atom. This contrasting behavior of the charges of the "Y" and hydrogen atoms in the ethene and benzene complexes distinguishes the π−H interaction exhibited by olefinic and aromatic π systems. In the case of the BH_3 complexes, the significant amount of charge transfer from the π system to the boron atom can be attributed to the π-p_z interaction.[37] Except for the complexes of HF, these charge shifts cannot be correlated to the electrostatic energies obtained in the energy decomposition.

3.3. Vibrational Spectra. In the case of a conventional hydrogen bond, correlations can been made between the stretching frequency shifts and the strength of the hydrogen bond.[11,54] In a recent paper on the interaction of the water dimer with different π systems, we had reported a correlation between the red-shifts observed in the O−H streching mode (associated with the π−H interaction of H_2O) and the electrostatic energies ($E^{(1)}_{elst}$).[48] Hence, we examine if such a correlation exists if different hydrides (BH_3, CH_4, NH_3, H_2O, HF) interact with π systems.

A comparison of some of these theoretically predicted frequencies and the experimentally obtained numbers of the H_2O complexes has recently been reported.[29] Hence, we only concentrate on highlighting the relative trends. It can be seen from Table 6 and Figure 4h that, as one progresses from CH_4 to HF, the blue-shifts of the Y−H stretching modes associated with the π−H interaction get transformed into red-shifts. Hobza et al. have shown that the blue-shift observed in the case of the CH_4 complexes is observed in a number of other complexes.[55] Similar to what is observed in case of the conventional hydrogen bond, the red-shifts observed in the case of the π−H interaction can be correlated to the electronegativity of the "Y" atom. In particular it can be seen from the similarity of Figure 4 c and h, that these red-shifts can be correlated to the inductive energies. Although the other attractive components such as electrostatic and dispersive energies also have major roles, we find that the sum of the induction ($E^{(2)}_{ind}$) and exchange-induction ($E^{(2)}_{exch-ind}$) (Figure 4c) is highly correlated to $\delta\nu_{Y-H}$ (Figure 4h). It can also be seen from Table 6 that these red-shifts are accompanied by an increase in the intensity of the Y−H stretch. This is due to the presence of induced dipoles, as a result of which the dipole moment of the complex is larger than the vector sum of the monomer's moments.

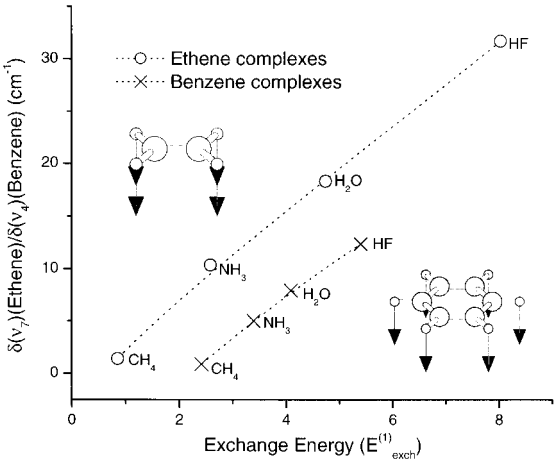

Figure 6. Correlation of the exchange energies ($E^{(2)}_{ind}$) with the out-of-plane bending shifts of ethene and benzene in all the complexes. The bending modes (ν_4, ν_7) are also shown in the graph.

It would thus be interesting to examine if any other frequency could be correlated to these energy terms. In Figure 6, a scatter plot of the calculated frequency shift associated with the highly IR active out-of-plane bending mode of both ethene and benzene, and the exchange energy ($E^{(2)}_{exch}$) is shown for all of the complexes exhibiting a π−H type of interaction. It can be seen that a linear relationship exists between both the out-of-plane bending-mode shifts and the exchange energies. This is supported from the fact that a decrease in the intermolecular distance leads to a drastic increase in the exchange-repulsion, and hence the consequent steepness of the potential surface at the equilibrium position leads to the blue-shifts. Since the decrease in the exchange energies directly influences the total interaction energy, a similar correlation between these out-of-plane bending shifts and the total interaction energies ($E^{(SAPT)}_{int}$) of these complexes can be obtained. It is of interest to note that Engdahl and Nelander obtained an estimate of the binding energy of the C_2H_4−H_2O complex using such a correlation.[56] Given the fact that the experimental binding energies of only the C_6H_2−H_2O complex have been determined,[57] we believe that such a correlation would be very useful in obtaining accurate experimental estimates of the binding energies of other complexes exhibiting a π−H interaction.

4. Conclusions

The present study details the interactions of the first-row hydrides with both the olefinic (ethene) and aromatic (benzene) π systems. The calculations carried out at both the MP2 and CCSD(T) level using reasonably large basis sets indicate that the binding energies of the benzene complexes are higher than those of the corresponding ethene complexes, with the exception of that of BH_3. The π−H interaction becomes stronger as one progresses from CH_4 to HF. The geometries obtained at these levels indicates that a π−H interaction is present only in complexes of CH_4, NH_3, H_2O, and HF with both benzene and ethene. The interaction observed in case of the C_2H_4−CH_4 complex cannot, however, be termed as a π−H interaction. While calculations using small basis sets seem to indicate that NH_3 can behave as a proton acceptor, those using larger basis sets clearly indicate that NH_3 is a proton donor. This indicates the importance of both large basis sets and high levels of correlation in the accurate description of these complexes.

(54) Badger, R. M.; Bauer, S. H. *J. Chem. Phys.* **1939**, *5*, 839.
(55) Hobza, P.; Špirko, V.; Havlas, Z.; Buchhold, K.; Reimann, B.; Barth, H.-D.; Brutschy, B. *Chem. Phys. Lett.* **1999**, *299*, 180; Hobza, P.; Špirko, V.; Selzle, H. L.; Schlag, E. W. *J. Phys. Chem. A* **1998**, *102*, 2501.
(56) Engdahl, A.; Nelander, B. *Chem. Phys. Lett.* **1983**, *100*, 129.
(57) Courty, A.; Mons, M.; Dimicoli, I.; Piuzzi, F.; Gaigeot, M.; Brenner, V.; de Pujo, P.; Millié, P. *J. Phys. Chem. A* **1998**, *102*, 6590.

We find that the exchange energies dramatically increase as we progress from NH_3 to HF, with the increase being much more pronounced in the ethene complexes. However, this increase is almost canceled out by both the electrostatic and dispersion energies in the case of the ethene complexes. Consequently, the induction energies become more important in the case of the ethene complexes. On the other hand, both electrostatic and induction energies seem to be important in the description of the benzene complexes. However, given the small magnitudes of the total binding energies involved, dispersion energies are also very important to obtain accurate values of the binding energies of all of these complexes. In particular, the inclusion of electron correlation is of vital importance in calculations involving π−H interaction, since otherwise the electrostatic, induction, and the dispersion energies are understimated.

An examination of the vibrational frequencies reveals that the shifts associated with the Y−H stretching modes get transformed from blue to red as one progresses from CH_4 to HF and can be correlated to the induction energy. On the other hand, no correlation can be made between the electrostatic energies and the stretching mode shifts. The highly IR active out-of-plane bending mode of the π system exhibits a chararacteristic blue-shift, which is reflective of exchange-repulsion and hence the strength of the π−H interaction.

Finally, it should be pointed out that electrostatic energies have a far more dominant role in the formation of a conventional hydrogen bond than a π H-bond. Both inductive and dispersion energies (the magnitude of which is dependent on the nature of the hydride) as well as the nature of the olefinic/aromatic π system have an important role in the formation of the π−H bond. As a result, the nature of the π system becomes very important in governing the binding energies of these complexes.

Acknowledgment. This work was supported by MOST/STEPI (CRIP). We thank Dr. Maciek Kolaski for helping us solve the problem of nonconvergence in case of the ethene−methane interaction. We thank Professor Krzysztof Szalewicz for providing us a copy of SAPT, his helpful comments on running SAPT for the large systems investigated in this study, and for his critical comments on our preliminary version of this manuscript.

Note Added in Proof. The reader's attention is directed to a highly germane reference that has recently appeared in print: Hydrogen Bonds with π-Acceptors in Proteins: Frequencies and Role in Stabilizing Local 3D Structures. Steiner, T.; Koellner, G. *J. Mol. Biol.* **2001**, *305*, 535−557.

Supporting Information Available: Cartesian coordinates (standard orientation) of the optimized geometries of all of the complexes evaluated at both the MP2/6-31+G* and MP2/aug-cc-pVDZ levels alongwith the corresponding MP2 energies in hartrees; Table S1 and S2 containing the binding energies and selected distances of the ethene and benzene complexes evaluated at the MP2/6-31+G* level; Table S3 containing the calculated MP2/6-31+G* frequency shifts of the Y−H stretching modes of all the complexes (PDF). This material is available free of charge via the Internet at http://pubs.acs.org.

JA0013531